

Shao-Yong Jiang · Yong-Quan Chen · Hong-Fei Ling ·
Jing-Hong Yang · Hong-Zhen Feng · Pei Ni

Trace- and rare-earth element geochemistry and Pb–Pb dating of black shales and intercalated Ni–Mo–PGE–Au sulfide ores in Lower Cambrian strata, Yangtze Platform, South China

Received: 8 June 2005 / Accepted: 31 March 2006 / Published online: 30 May 2006
© Springer-Verlag 2006

Abstract The Lower Cambrian black shale sequence of the Niutitang Formation in the Yangtze Platform, South China, hosts an extreme metal-enriched sulfide ore bed that shows >10,000 times enrichment in Mo, Ni, Se, Re, Os, As, Hg, and Sb and >1,000 times enrichment in Ag, Au, Pt, and Pd, when compared to average upper continental crust. We report in this paper trace- and rare-earth-element concentrations and Pb–Pb isotope dating for the Ni–Mo–PGE–Au sulfide ores and their host black shales. Both the sulfide ores and their host black shales show similar trace-element distribution patterns with pronounced depletion in Th, Nb, Hf, Zr, and Ti, and extreme enrichment in U, Ni, Mo, and V compared to average upper crust. The high-field-strength elements, such as Zr, Hf, Nb, Ta, Sc, Th, rare-earth elements, Rb, and Ga, show significant inter-element correlations and may have been derived mainly from terrigenous sources. The redox sensitive elements, such as V, Ni, Mo, U, and Mn; base metals, such as Cu, Zn, and Pb; and Sr and Ba may have been derived from mixing of seawater and venting hydrothermal sources. The chondrite-normalized REE patterns, positive Eu and Y anomalies, and high Y/Ho ratios for the Ni–Mo–PGE–Au sulfide ores are also suggestive for their submarine hydrothermal-exhalative origin. A stepwise acid-leaching Pb–Pb isotope analytical technique has been employed for the Niutitang black shales and the Ni–Mo–PGE–Au sulfide ores, and two Pb–Pb isochron ages have been obtained for the black shales (531 ± 24 Ma) and for the Ni–Mo–PGE–Au sulfide ores

(521 ± 54 Ma), respectively, which are identical and overlap within uncertainty, and are in good agreement with previously obtained ages for presumed age-equivalent strata.

Keywords Trace- and rare-earth elements · Pb–Pb dating · Ni–Mo–PGE–Au sulfide ore · Black shale · South China

Introduction

Black shale is an important host for redox-sensitive metals, such as Mo, Ni, V, U, Re, and a number of other metals including Cu, Pb, Zn, Au, Ag, Hg, Sb, etc. in various geological periods and settings (Holland 1979; Coveney et al. 1992; Pasava 1993). Metal-enriched black shale of Early Cambrian age occurs over several thousands of kilometers throughout the Yangtze Platform in South China. The lowermost part of this black shale formation contains a thin Ni–Mo sulfide ore horizon with Ni and Mo contents in the weight percent (wt%) range. This sulfide ore bed and its host black shale also show exceptional enrichments in a suite of redox-sensitive metals (e.g., U, V, Re), noble metals (e.g., Pd, Pt, Au, Ag), and many other metals, such as Se, As, Hg, Sb, Ag, and Au (Fan et al. 1973, 1984; Murowchick et al. 1994; Lott et al. 1999). Although this type of metal enrichment has been known for >30 years, its origins still remain to be resolved definitively. These ores are important in particular, because they constitute a largely untested alternative to conventional sources of platinum group elements and gold. Two major models have been proposed: one is of submarine hydrothermal exhalative origin (Coveney et al. 1992; Lott et al. 1999; Steiner et al. 2001; Coveney 2003), and another is of seawater precipitation/scavenging origin (Mao et al. 2002; Lehmann et al. 2003). To better understand the origin for the Ni–Mo–PGE–Au sulfide ores and to constrain the mineralization age, we conducted a trace- and rare-earth-element study and Pb–Pb isotope dating for the ores and black shales from the Lower Cambrian strata in the Yangtze Platform of South China, with preliminary results presented in this paper.

Editorial handling: R. Coveney Jr.

S.-Y. Jiang (✉) · Y.-Q. Chen · H.-F. Ling ·
J.-H. Yang · H.-Z. Feng · P. Ni
State Key Laboratory for Mineral Deposits Research
and Center for Marine Geochemistry Research,
Department of Earth Sciences, Nanjing University,
Nanjing 210093, People's Republic of China
e-mail: shyjiang@nju.edu.cn

Geological setting and general description of the Ni–Mo sulfide ore

In the Yangtze platform of south China, Neoproterozoic and Early Cambrian strata are well exposed. The depositional facies range from shallow-water settings of carbonates and phosphorites to transitional and deeper-water environments represented by black shales and cherts (Zhu 2004). The Ni–Mo–PGE–Au sulfide ore bed occurs in the Lower Cambrian black shale sequence of the Niutitang Formation and stratigraphic equivalents along a 1,600-km long narrow NE striking belt of transitional and deeper water facies along the margins of the Yangtze platform (Fig. 1) (Fan 1983; Fan et al. 1973, 1984; Mao et al. 2002; Zhu 2004).

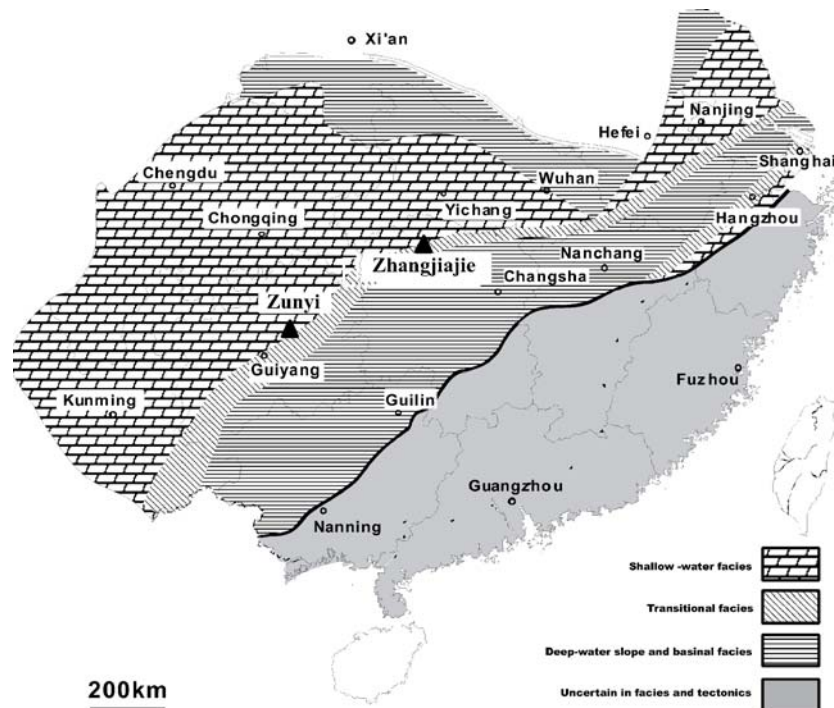
Metal enrichments in the Ni–Mo–PGE–Au sulfide ores include Mo, Ni, Se, Re, Os, As, Hg, Sb, Ag, Au, Pt, and Pd (Fan et al. 1973; Murowchick et al. 1994; Li and Gao 1999; Steiner et al. 2001; Mao et al. 2002). The enrichment factor of these metals, compared to seawater, is on the order of 10^6 to 10^9 (Mao et al. 2002). When compared to average upper continental crust (Taylor and McLennan 1985), metals such as Mo, Ni, Se, Re, Os, As, Hg, and Sb show >10,000 times enrichment, and metals such as Ag, Au, Pt, and Pd are more than 1,000 times enriched (Mao et al. 2002). Although the ore-bearing black shale sequence occurs sporadically over a 1,600-km length covering six provinces in southeast China, the economically minable ores are exposed mostly within the Guizhou and Hunan provinces, with the most famous occurrences at Zunyi of Guizhou province and Zhangjiajie of Hunan province.

The Ni–Mo sulfide orebodies have restricted, lenticular, and bedded shape and are located at approximately the same stratigraphic horizon within the lowermost Niutitang

black shale formation. The thickness of the ore bed is commonly a few centimeters, but locally can be up to tens of centimeters, even 1–2 m (e.g., Huangjiawan mine in Zunyi; Zeng 1998). The ore minerals mainly consist of MoSC phase ($[Mo, Fe, Ni][S, As]_2C_7$), vaesite, bravoite, and jordisite (Kao et al. 2001), with minor sulfide components of arsenopyrite, chalcopyrite, covellite, sphalerite, millerite, polydymite, gersdorffite, sulvanite, pentlandite, tennantite, tiemannite, violarite, and native Au (Fan 1983; Kao et al. 2001; Coveney et al. 1994; Lott et al. 1999). The ore type includes laminated and nodular ores. The laminated ores are dominant, which include metal-rich sulfide layers intercalated with metal-poor siliceous–carbonaceous layers. The gangue minerals contain illite, sericite, quartz, calcite, barite, apatite, and collophane. The nodular ore consists of <1–3 mm nodules of a mixture of a heterogeneous micro-crystalline assemblage of Ni–Mo sulfides, a colloid-like Mo–S–C phase, and organic debris, siliceous rock, carbonate, clay, and phosphorite.

In Guizhou and Hunan provinces, the lowermost Ni–Mo sulfide-bearing Niutitang Formations commonly consist of stratiform cherts, nodular and bedded phosphorites, and organic carbon-rich black shales (Fig. 2). The black shales in the lower part of the Niutitang Formation have generally higher TOC (up to 15 wt%) contents than the upper unit that contain on average 3–9 wt% TOC (Steiner et al. 2001). The Niutitang Formation rests unconformably on the Neoproterozoic Dengying Formation of dolomite following a stratigraphic hiatus (Fig. 3). The Dengying dolomite is underlain by the Doushantuo Formation, a sequence of black shale, chert, phosphorite, and dolomite, with recent Pb–Pb dating of 576 ± 14 Ma for the upper part and 599 ± 4 Ma for the lower part of the Upper Phosphorite Bed (Barfod et al. 2002; Chen et al. 2004). Three zircon SHRIMP

Fig. 1 Simplified geological map showing distribution of Neoproterozoic–Cambrian paleoceanographic facies in Yangtze Platform (modified after Zhu 2004). The Ni–Mo–PGE–Au sulfide ore bed and black shales occur in a narrow belt of transitional and deeper water facies along the margins of the Yangtze Platform, with the most important occurrences at Zunyi of Guizhou province and Zhangjiajie of Hunan province



U–Pb ages (628.3±15.8 Ma; 621±7 Ma; and 555.2±6.1 Ma) from distinctive volcanic ash beds were also reported recently, which placed excellent constraints on the duration of the Doushantuo Formation (Yin et al. 2005; Zhang et al. 2005). The Doushantuo Formation in turn rests on diamictite of the Nantuo Formation, which is considered as glaciogenic rock, and is correlated with the Neoproterozoic Marinoan ice age at about 630 Ma (Gradstein et al. 2004). The entire sedimentary sequence is thought to represent a sedimentary shelf environment characterized by repeated transgression–regression episodes on the Lower Proterozoic–Archean Yangtze craton (Quip et al. 2000; Steiner et al. 2001).

Analytical methods

We analyzed trace- and rare-earth-element concentrations, and Pb–Pb isotopic compositions of the Niutitang black shales from Zunyi of Guizhou province, and the Ni–Mo–PGE–Au sulfide ores from Zunyi of Guizhou province and Zhangjiajie of Hunan province.

The black shale samples for trace- and rare-earth-element analysis were dissolved using a reverse *aqua regia* (2:1 conc. HNO₃/conc. HCl) in an Anton Paar High Pressure Asher HPA-S instrument at high temperature

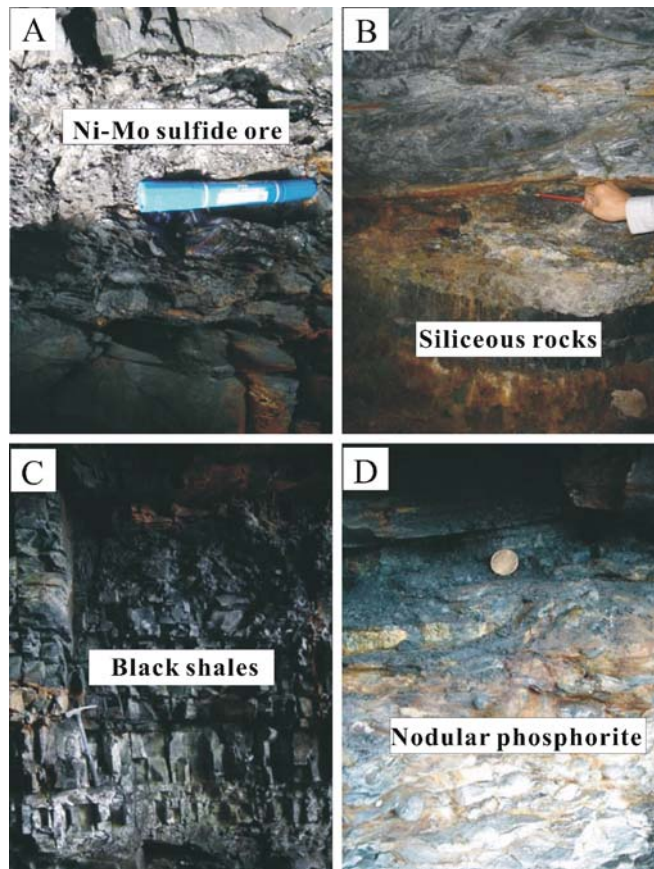


Fig. 2 Field photos showing cherts, nodular phosphorites, Ni–Mo ore layer, and organic carbon-rich black shales. All photos were taken from Sancha section at Zhangjiajie, Hunan province

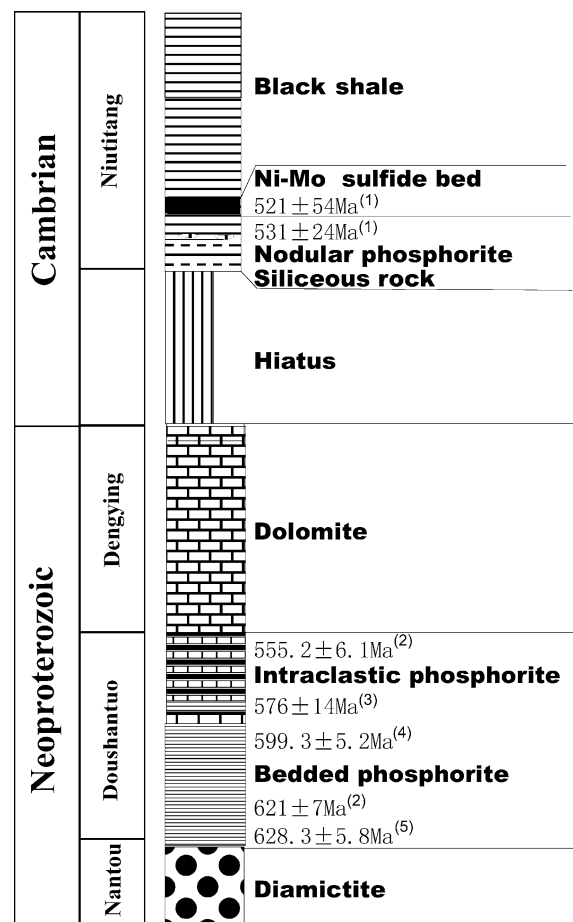


Fig. 3 Composite section showing Neoproterozoic to Early Cambrian stratigraphic lithology in the studied areas of Guizhou and Hunan provinces. The corresponding isotope ages are from (1) this study, (2) Zhang et al. (2005), (3) Chen et al. (2004), (4) Barfod et al. (2002), and (5) Yin et al. (2005)

(320°C) and high pressure (130 bar). This technique is very efficient for complete dissolution of organic-carbon-rich samples, such as black shales. The dissolved solutions were centrifuged and separated from the detritus. The Ni–Mo–PGE–Au sulfide ores for trace- and rare-earth-element analysis were dissolved using a stepwise acid-leaching technique. We used 1 N HCl (step A), 2 N HBr + 2.5 N HCl (step B), conc. HNO₃ + conc. HCl (step C), and conc. HF + conc. HNO₃ (step D) to leach the ore samples. Compared to the host black shales, the Ni–Mo–PGE–Au sulfide ores contain more complex mineral assemblages that may have formed during different stages. Therefore, the stepwise acid-leaching technique applied may reveal detailed information regarding various ore-formation stages or sources. The carbonates, phosphorites, and some monosulfides may have been largely leached out during step A. Most sulfide minerals are leached by steps B and C. The minor siliceous materials and possibly other acid-resistant components are finally dissolved during step D. The sample solutions from both black shales and Ni–Mo–PGE–Au sulfide ores were spiked with 10 ppb Rh and made up to 50 ml in 5% HNO₃ solution. These solutions were then measured using a Finnigan HR-ICP-MS at the State Key

Laboratory for Mineral Deposits Research, Nanjing University. The analytical precision of the samples is better than 10%. The results are listed in Tables 1 and 2.

The Pb isotopic compositions of black shales and Ni–Mo–PGE–Au sulfide ores were measured using a TIMS (Finnigan Triton TI) at the State Key Laboratory for Mineral Deposits Research, Nanjing University. The sample preparation employed a stepwise acid-leaching procedure of 1 N HCl (step A), 2 N HBr + 2.5 N HCl (step B), and conc. HNO₃ + conc. HCl (step C) in an attempt to release Pb bound in different minerals or mineral structures (e.g., carbonates, sulphides, organic carbon, clay minerals, etc.). The purpose of the stepwise acid-leaching technique is to extend the range of Pb-isotopic ratios to yield a more precise Pb–Pb isochron date. The acid-leaching Pb-isotopic compositions should represent a combination of the Pb-isotope signature of Cambrian seawater or ore-forming solutions and radiogenic lead from decay of U that was incorporated into the black shales or Ni–Mo–PGE–Au sulfide ores during deposition. The solutions collected in each leaching step were mixed with HBr and then dried. After redissolution, Pb was then separated and purified using anion resin (Biorad AG1X8, 200–400 mesh) following the methods of Galer and O’Nions (1989). The Pb samples were loaded on single Re filaments with a conventional silicon gel and phosphorous acid technique, and the Pb-isotope ratios were then measured by thermal ionization mass spectrometry. Several standards of NIST Pb-981 were analyzed during each set of sample measurement. All measurements of samples and standards were performed at similar temperatures of ~1250°C and for similar time duration. Pb-isotopic compositions of the samples analyzed are presented in Table 3 after correction for mass fractionation based on the measured results and published values of NIST Pb-981 standard (Todt et al. 1996).

Pb–Pb dating of black shales and Ni–Mo–PGE–Au sulfide ores

The Pb–Pb dating of black shales and Ni–Mo–PGE–Au sulfide ores from the Lower Cambrian Niutitang Formation yields isochron ages of 531±24 Ma ($n=34$, MSWD=1.6) and 521±54 Ma ($n=9$, MSWD=31), respectively (Figs. 4, 5). The two ages are similar and overlap within uncertainty, and are in good agreement with previously obtained ages for presumed age-equivalent strata. For example, the biostratigraphic age of the Niutitang Formation is constrained by a pretrilobitic fauna consisting of arthropods, sponges, and small shelly fossils of Tommotian age of about 530 Ma (Steiner et al. 2001). Horan et al. (1994) and Mao et al. (2002) reported Re–Os ages for the Ni–Mo–PGE–Au sulfide ores of 560±50 and 541±16 Ma, respectively. Li et al. (2002) also reported a Re–Os isochron age of 542±11 Ma for the Ni–Mo–PGE–Au sulfide ores. Murowchick et al. (1992) also obtained a Pb–Pb age of 551±52 Ma for the same Ni–Mo–PGE–Au sulfide ores. Jenkins et al. (2002) reported a SHRIMP U–Pb age of

538.2±1.5 Ma for zircon from tuff within Bed 5 of the basal Cambrian Meishucun Formation, South China. Although the age-equivalent Meishucun Formation does not occur in the sections we studied, the Niutitang Formation appears younger than the Meishucun Formation. Therefore, the above-mentioned ages of 541 to 560 Ma are slightly older than the actual depositional age of the Niutitang Formation. Jiang et al. (2003) suggested that a Re–Os isochron age of 537±10 Ma should better represent the age of ore formation and black shale deposition in the Niutitang Formation, which is in good agreement with the Pb–Pb isotope age of 531±24 Ma (Chen et al. 2003).

The direct dating of sedimentary rocks has been an important subject in isotope geochemistry, and has been considered as a difficult task (Stille and Clauer 1986; Gauthier-Lafaye et al. 1996). The Rb–Sr, Sm–Nd, and K–Ar isotope systems have been previously used to date deposition and early diagenesis in shale sequences but with only limited success (Clauer 1981; Stille and Clauer 1986; Bros et al. 1992). Recently, the Pb–Pb isotope system for sedimentary rocks, such as black shales and phosphorites has been proven to hold great promise to date depositional or early diagenetic ages. Gauthier-Lafaye et al. (1996) presented a first dating attempt of diagenetic clay minerals from Proterozoic black shales of the Franceville basin in Gabon and obtained a Pb–Pb isochron age of 2328±130 Ma (MSWD=1.24), which is identical with a previous Sm–Nd isochron age. In their experiments, they leached diagenetic clay minerals extracted from black shales with 1 N HCl, and suggested that the leachates are the most appropriate phases for Pb isotope dating. Barfod et al. (2002) employed an acid-leaching method to obtain a Pb–Pb isochron age of 599.3±4.2 Ma for the lower part of the Upper Phosphorite Bed in the Neoproterozoic Doushantuo Formation from Weng’an and Kaiyang, Guizhou Province, which is identical to the Lu–Hf isochron age (584±26 Ma) of the same phosphorites. Chen et al. (2004) further obtained a Pb–Pb isochron age of 576±14 Ma for the upper part of the Upper Phosphorite Bed in the Neoproterozoic Doushantuo Formation. Our study also demonstrates that the Pb–Pb isochron technique is valid to approximate the depositional age of the black shales and sulfide ores (Chen et al. 2003).

Trace-element geochemistry

Trace-element concentrations and ratios have been widely used to constrain the genesis of submarine hydrothermal ore deposits (e.g., Whitehead et al. 1992; Canet et al. 2004; Jiang et al. 1999, 2005). The Ni–Mo–PGE–Au sulfide ores and their host black shales in the Lower Cambrian Niutitang Formation show a broadly similar trace-element-distribution pattern with average upper crust normalization (Rollinson 1993). Both sets of samples are depleted in Th, Nb, Hf, Zr, and Ti, and enriched in U, Ni, Mo, and V, although the degree of depletion/enrichment in the sulfide ores is much more pronounced (Fig. 6). The black shales also show a characteristic depletion in Sr, but the sulfide

Table 1 Trace- and rare-earth-element concentrations (in ppm) of black shales in the Lower Cambrian Niutitang Formation, South China

	GZW27	GZW28	GZW29	GZW30	ZN28	ZN29	ZN30	ZN31	ZN32	ZN33	ZN34	ZN35	ZN35-1
Li	76.1	48.9	42.2	42.1	991	1024	848	111	113	117	112	157	132
Be	13.8	7.03	6.47	7.94	16.2	19.1	4.29	10.3	8.90	9.41	7.64	7.45	6.86
Sc	41.8	37.5	31.7	34.7	17.1	21.6	14.9	38.5	22.3	24.7	23.6	31.4	33.3
Ti	2,263	2,299	1,923	1,849	1,774	1,492	1,629	1,458	643	2,103	2,206	2,126	2,005
V	684	405	372	417	254	538	1,234	8,232	3,168	8,603	11,339	15,652	16,515
Cr	258	239	218	186	335	218	372	397	1,591	5,157	5,686	2,455	3,153
Mn	325	1,146	977	1,142	184	23.4	81	18.9	170	126	70.5	61.7	89.2
Co	75.6	43.8	39.7	42.4	6.66	0.21	1.80	0.26	0.83	3.53	4.03	5.96	4.89
Ni	278	191	176	144	167	26.1	186	42.6	124	254	308	399	337
Cu	1,121	809	732	519	586	140	524	731	379	434	1,392	312	187
Zn	1,001	819	761	385	261	114	259	443	357	774	1,490	3,189	2,318
Ga	59.7	48.0	43.8	48.9	52.4	54.9	25.5	111	33.1	37.4	33.9	47.2	47.7
Rb	393	315	278	314	241	305	104	481	237	279	235	314	317
Sr	101	104	88.9	108	50.8	57.2	168	56.7	229	64.3	74.9	74.4	70.4
Y	62.8	57.1	51.4	54.9	22.7	26.7	50.1	185	66.9	262	163	90.6	132
Zr	207	158	138	155	209	236	86.1	235	89.8	161	120	121	133
Nb	2.45	2.61	2.53	2.43	4.61	8.70	13.9	46.9	0.56	4.75	3.76	2.21	1.86
Mo	79.7	26.2	25.6	23.3	173	41.9	70.2	53.9	74.4	80.5	132	315	261
Sn	7.20	6.77	6.25	6.26	11.9	10.7	6.05	30.1	1.32	8.28	5.93	7.69	6.61
Cs	49.3	36.1	33.2	37.4	22.7	41.8	10.9	31.8	22.5	32.5	28.7	36.9	41.3
Ba	1,033	870	787	936	659	5,231	13,686	11,384	4,804	5,276	5,919	7,163	6,497
Hf	3.73	3.79	3.27	3.91	5.42	5.28	1.85	10.04	1.73	3.97	2.70	3.07	3.40
Ta	0.01	0.01	0.02	0.02	0.01	0.03	0.01	0.01	0.02	0.02	0.05	0.04	0.01
W	1.26	1.37	1.24	1.00	0.40	0.38	0.44	0.21	0.13	0.13	0.66	0.89	0.57
Pb	207	142	142	163	75.2	23.3	32.2	21.3	27.5	30.4	36.1	44.3	51.8
Bi	1.22	0.87	0.86	0.90	0.92	1.29	0.42	2.31	1.34	1.65	1.39	1.03	1.01
Th	23.7	22.2	22.5	22.9	7.33	11.1	18.3	69.2	19.5	22.8	22.6	28.4	26.9
U	25.5	13.1	13.0	11.6	21.5	41.2	31.6	80.9	57.1	81.0	71.5	66.7	80.9
La	127.8	87.18	79.77	85.14	24.10	23.41	21.09	134.6	19.01	113.5	123.2	94.10	111.4
Ce	201.9	155.7	138.6	159.1	22.12	24.69	28.82	269.3	31.00	122.3	138.3	123.5	149.8
Pr	21.51	17.61	16.25	18.85	2.74	5.80	5.64	35.95	6.08	23.12	24.02	18.85	22.97
Nd	79.81	61.90	58.91	69.91	11.01	30.46	29.16	145.42	31.75	93.46	95.60	74.14	90.54
Sm	12.08	10.39	9.79	11.44	1.87	4.27	7.14	33.52	7.33	18.59	18.32	13.51	16.14
Eu	2.42	2.10	2.01	2.18	0.33	0.72	1.68	2.86	1.71	3.63	3.97	2.94	3.55
Gd	11.73	10.01	9.12	10.41	1.89	1.96	8.12	32.33	9.49	22.71	20.13	13.51	17.24
Tb	1.55	1.37	1.29	1.45	0.23	0.19	1.06	5.23	1.19	3.45	2.96	1.82	2.39
Dy	10.67	9.56	9.00	9.58	1.91	2.01	7.47	37.33	8.49	26.20	21.39	13.09	17.58
Ho	2.19	2.07	1.94	2.01	0.59	0.68	1.71	7.84	1.99	6.68	5.13	3.04	4.03
Er	6.13	6.06	5.67	5.86	2.68	3.38	5.23	22.53	6.13	20.49	15.69	9.05	11.92

Table 1 (continued)

	GZW27	GZW28	GZW29	GZW30	ZN28	ZN29	ZN30	ZN31	ZN32	ZN33	ZN34	ZN35	ZN35-1
Tm	0.94	0.85	0.81	0.82	0.59	0.83	0.79	3.03	0.87	3.02	2.29	1.41	1.82
Yb	5.97	5.09	5.12	5.13	4.76	6.81	5.45	17.26	5.56	17.51	13.40	8.17	10.58
Lu	0.94	0.72	0.76	0.76	0.82	1.27	0.87	2.39	0.86	2.56	1.88	1.23	1.59
Ce/Ce*	0.73	0.82	0.79	0.85	0.43	0.47	0.58	0.87	0.68	0.49	0.51	0.60	0.61
Eu/Eu*	0.62	0.63	0.65	0.61	0.54	0.76	0.67	0.27	0.63	0.54	0.63	0.66	0.65
La _N /Yb _N	14.43	11.55	10.50	11.18	3.41	2.32	2.61	5.26	2.30	4.37	6.20	7.77	7.10
Gd _N /Yb _N	1.58	1.59	1.44	1.64	0.32	0.23	1.20	1.51	1.38	1.05	1.21	1.34	1.32

Ce/Ce* represents Ce anomaly and has been expressed by Toyoda and Masuda (1991) as $5 \text{Ce}_{\text{N}}/(4 \text{La}_{\text{N}} + \text{Sm}_{\text{N}})$. The Eu anomaly (Eu/Eu*) is defined using the expression of McLennan (1989) as $\text{Eu}_{\text{N}}/(\text{Sm}_{\text{N}} \times \text{Gd}_{\text{N}})^{0.5}$.

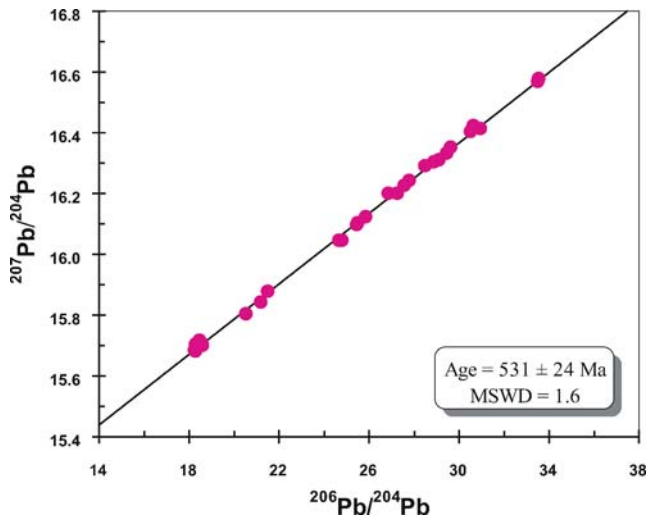


Fig. 4 Pb-Pb dating of black shales of the Lower Cambrian Niutitang Formation, South China

ores have no Sr depletion (Fig. 6). Positive linear correlations are shown for the high-field-strength elements such as Zr, Hf, Nb, Ta, Sc, Th, rare-earth elements, Rb and Ga both in the black shales and the Ni–Mo–PGE–Au sulfide ores (Fig. 7). These elements are generally regarded as immobile, and the inter-element correlations generally reflect mixing of variable mineral sources due to the preferential occurrence of these elements in stable Fe–Ti oxides and aluminosilicate minerals (Slack and Hoy 2000).

The redox-sensitive elements, such as V, Ni, Mo, U, and Mn, base metals, such as Cu, Zn, Pb, as well as Sr and Ba, are generally regarded as derived from hydrothermal sources and/or precipitated under euxinic (anoxic and sulfidic) conditions in marine environments. These elements show distinctly different distribution patterns between black shales and the Ni–Mo–PGE–Au sulfide ores, and only a broad linear correlation has been observed for some of the element pairs, such as Cu–Zn, Mo–U, and

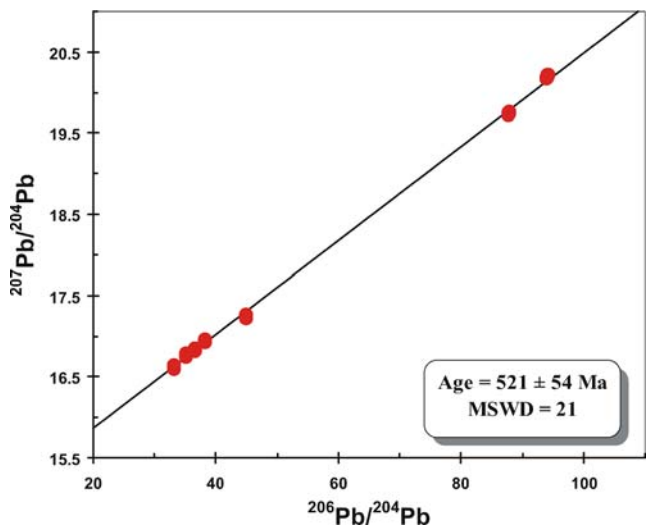


Fig. 5 Pb-Pb dating of Ni–Mo–PGE–Au sulfide ores in the Lower Cambrian Niutitang Formation, South China

Table 2 Trace- and rare-earth-element concentrations (in ppm) of Ni–Mo–PGE–Au sulfide ores in the Lower Cambrian Niutitang Formation, South China

	HN-1a	HN-1b	HN-1c	HN-1d	HN-2a	HN-2b	HN-2c	HN-2d	GZ-1a	GZ-1b	GZ-1c	GZ-1d
Li	0.71	0.22	0.41	29.5	0.97	0.32	0.16	34.7	0.83	0.22	11.0	5.40
Be	0.04	0.03	0.17	0.05	0.10	0.00	0.15	0.11	0.16	0.02	0.29	0.05
Sc	0.97	0.10	0.30	0.35	0.87	0.18	0.30	0.46	1.49	0.09	0.61	0.40
Ti	3.55	10.22	61.9	396	1.72	4.21	51.9	444	4.47	4.57	41.1	336
V	52.8	14.9	358	149	25.4	10.4	152	102	64.4	7.65	283	97
Cr	22.9	6.73	39.7	17.6	13.1	6.50	23.2	16.8	1.60	0.30	14.7	6.11
Mn	92.2	4.93	50.6	3.95	97.6	10.4	28.2	3.15	759	54.2	18.9	2.10
Co	9.62	0.45	42.6	3.52	8.49	0.57	41.8	3.66	2.72	0.88	9.80	0.41
Ni	9,237	615	7,381	595	8,789	751	9,792	688	578	53.5	1,494	64.1
Cu	814	68.7	248	24.0	429	74.9	451	40.4	62.4	6.79	199	9.02
Zn	1,284	204	390	39.7	1,739	194	374	39.7	162	101	235	18.6
Ga	0.40	0.07	2.20	3.17	0.78	0.20	2.13	4.30	0.72	0.14	3.13	1.66
Rb	0.41	0.26	1.37	5.95	0.43	0.27	1.24	7.36	0.52	0.37	12.35	9.05
Sr	46.2	3.87	7.44	2.17	142	22.2	4.04	2.10	324	17.6	17.9	7.74
Y	38.2	1.68	1.47	0.22	105.0	12.34	1.86	0.29	62.3	3.62	3.16	1.94
Zr	1.06	0.99	4.98	11.0	0.40	0.43	4.71	11.1	2.06	1.00	6.27	11.9
Nb	0.02	0.02	0.17	1.19	0.01	0.01	0.15	1.37	0.01	0.01	0.07	0.92
Mo	2,027	552	26,973	1,407	1,203	490	19,677	1,007	369	76.8	418	16.6
Sn	0.63	0.02	1.30	0.37	0.35	0.01	1.00	0.40	0.19	0.01	0.32	0.12
Cs	0.34	0.42	3.36	0.28	0.27	0.26	0.98	0.22	0.06	0.10	1.22	0.26
Ba	27.0	66.6	40.3	128	40.0	25.0	8.64	119	134	157	354	173
Hf	0.03	0.02	0.09	0.29	0.03	0.01	0.09	0.29	0.05	0.02	0.13	0.28
Ta	0.003	0.002	0.003	0.052	0.006	0.001	0.005	0.046	0.004	0.001	0.001	0.035
W	0.35	0.39	7.88	2.07	0.08	0.07	6.73	1.78	0.24	0.15	0.46	0.10
Pb	61.4	5.75	137	8.05	55.7	9.79	86.8	6.46	3.78	0.36	2.00	0.73
Bi	2.07	0.20	2.82	0.14	3.12	0.49	6.18	0.25	0.30	0.06	0.24	0.01
Th	1.13	0.17	0.23	0.10	0.97	0.45	0.13	0.08	1.52	0.30	0.46	0.09
U	57.2	16.6	90.6	5.72	61.9	34.2	123	6.80	28.5	17.3	20.5	2.82
La	17.58	1.03	0.65	0.10	41.42	7.19	0.89	0.13	40.50	3.58	3.13	0.40
Ce	23.71	1.48	0.95	0.33	52.63	11.47	1.35	0.46	56.87	4.04	3.87	2.36
Pr	3.08	0.21	0.15	0.02	8.50	1.67	0.18	0.02	6.85	0.42	0.40	0.06
Nd	12.86	0.88	0.59	0.07	38.43	7.36	0.74	0.08	29.17	1.61	1.45	0.18
Sm	2.29	0.16	0.13	0.02	7.63	1.38	0.17	0.02	5.51	0.27	0.20	0.03
Eu	0.73	0.05	0.03	0.01	2.07	0.34	0.03	0.01	2.45	0.16	0.09	0.02
Gd	2.89	0.18	0.12	0.02	10.08	1.53	0.14	0.02	6.60	0.31	0.22	0.06
Tb	0.46	0.03	0.02	0.002	1.51	0.21	0.03	0.003	0.94	0.05	0.04	0.01
Dy	3.05	0.16	0.03	0.03	9.07	1.23	0.22	0.03	5.48	0.33	0.26	0.15
Ho	0.67	0.03	0.04	0.01	1.82	0.23	0.05	0.01	1.06	0.07	0.06	0.04
Er	1.93	0.10	0.13	0.03	4.80	0.61	0.17	0.03	2.91	0.24	0.22	0.14

Table 2 (continued)

	HN-1a	HN-1b	HN-1c	HN-1d	HN-2a	HN-2b	HN-2c	HN-2d	GZ-1a	GZ-1b	GZ-1c	GZ-1d
Tm	0.23	0.02	0.03	0.00	0.51	0.07	0.04	0.01	0.34	0.03	0.04	0.02
Yb	1.13	0.10	0.20	0.04	2.43	0.36	0.27	0.05	1.72	0.20	0.25	0.14
Lu	0.15	0.01	0.02	0.01	0.31	0.04	0.03	0.01	0.23	0.03	0.03	0.02
Ce/Ce*	0.61	0.65	0.65	1.47	0.57	0.71	0.68	1.56	0.64	0.53	0.58	2.73
Eu/Eu*	0.87	0.98	0.67	2.78	0.72	0.71	0.60	2.20	1.24	1.69	1.38	1.44
La _N /Yb _N	10.44	6.87	2.24	1.73	11.50	13.37	2.22	1.94	15.84	12.22	8.59	2.00
Gd _N /Yb _N	2.06	1.42	0.51	0.32	3.35	3.40	0.43	0.27	3.09	1.27	0.71	0.39

Mo–V in the sulfide ores (Fig. 8). The redox sensitive elements are usually highly enriched in anoxic and sulfidic depositional conditions. Black shales usually contain elevated Mo (Wignall 1994). In the Black Sea, sapropelic muds have Mo concentrations up to 188 ppm (Hirst 1974).

Black shales of the Niutitang Formation also show high Mo contents up to several hundreds of ppm (Table 1), not to mention the intercalated Ni–Mo–PGE–Au sulfide ores within the Niutitang black shale that may contain up to 9.3 wt% Mo (Mao et al. 2002). The Mo contents are broadly correlated with the U contents, both in the black shales and the sulfide ores (Fig. 8), which are well in accordance with anoxic bottom water conditions. Soluble uranium in its oxidized state must be reduced and fixed as tetravalent U in the sediments of anoxic basins, as opposed to its unreactive behavior in oxic marine basins (Anderson et al. 1989). The precipitation of U in the sediments drives diffusion of U into pore waters, and U is enriched in organic-rich sediments.

Mn is also an effective indicator of bottom water conditions due to the sensitivity of its solubility to redox changes. Marine sediments deposited under oxygenated condition show relatively high Mn contents because Mn⁴⁺ precipitates readily as an oxyhydroxide. During reducing and anoxic conditions, Mn can be dissolved from the bottom sediment and diffused into the overlying anoxic water column, leading to concentrations that are depleted with respect to average shale (Yarincik et al. 2000). Sediments from the Black Sea and Selwyn Basin that formed under anoxic conditions are commonly depleted in Mn (Cooper et al. 1974; Goodfellow and Jonasson 1986). The broad negative correlation between Mn and V for the Niutitang black shales (Fig. 8) may reflect changing redox conditions during their deposition, as has been demonstrated by Quinby-Hunt and Wilde (1994) that black shales characterized by lower Mn and higher V contents may have formed under more reducing conditions.

Rare-earth-element geochemistry

Rare-earth elements are effective indicators for depositional environments and ore genesis of submarine hydrothermal exhalative deposits (i.e., Graf 1977; Lottermoser 1989; Steiner et al. 2001). Figure 9 shows chondrite-normalized REE distribution patterns of the Niutitang black shales. The data show a slightly light rare-earth (LREE) enrichment and middle rare-earth (MREE) depletion with chondrite-normalized La_N/Yb_N and Gd_N/Yb_N ratios of 2.3–14.4 and 0.23–1.64, respectively (Table 1). The two samples with the lowest total REE contents show the strongest MREE depletion with a V-shaped REE pattern (Fig. 9). Moderate to strong negative Eu and Ce anomalies are evident for most of the black shale samples with Eu/Eu* and Ce/Ce* values of 0.27–0.76 and 0.43–0.87, respectively. The Ni–Mo–PGE–Au sulfide ores show similar degree of LREE enrichment but lesser degree of MREE depletion, compared to the black shales with La_N/Yb_N and Gd_N/Yb_N ratios of 1.7–15.8 and 0.27–3.4,

Table 3 Pb isotopic compositions of black shales and Ni–Mo–PGE–Au sulfide ores in the Lower Cambrian Niutitang Formation, South China

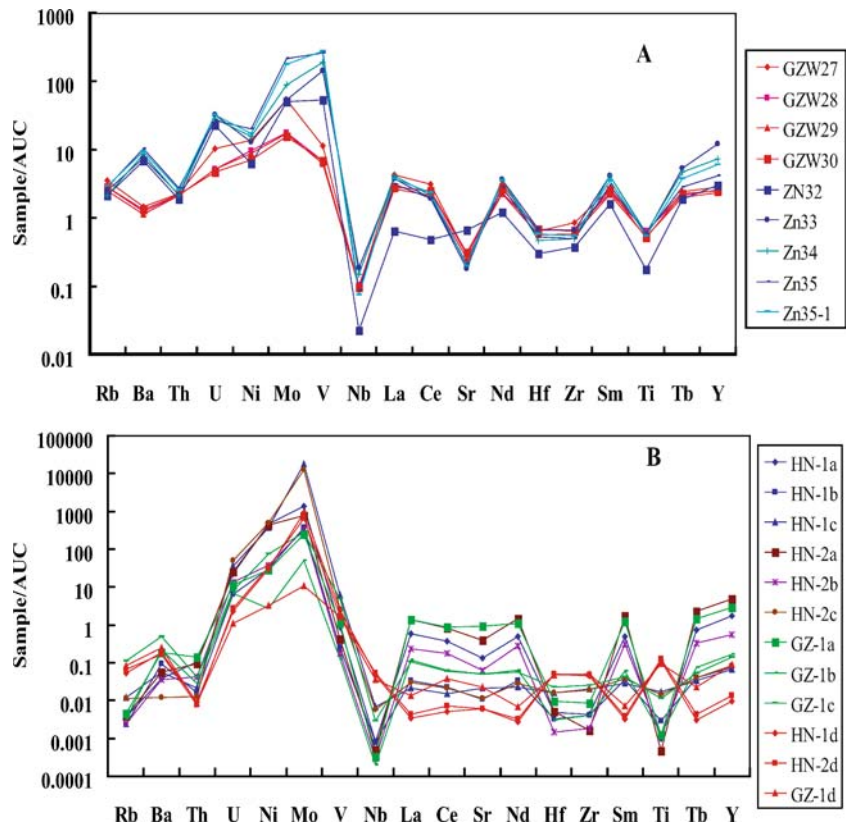
Sample no.	Sample type	Leaching step	$^{206}\text{Pb}/^{204}\text{Pb}$	$^{207}\text{Pb}/^{204}\text{Pb}$	$^{208}\text{Pb}/^{204}\text{Pb}$
GZW-27	Black shale	a	18.592	15.708	38.289
		b	18.597	15.701	38.222
		c	18.488	15.716	38.263
GZW-28	Black shale	a	18.361	15.699	38.303
		b	18.354	15.689	38.264
		c	18.384	15.696	38.256
GZW-29	Black shale	a	18.298	15.691	38.269
		b	18.293	15.681	38.231
		c	18.338	15.693	38.250
GZW-30	Black shale	a	18.299	15.703	38.330
		b	18.280	15.683	38.262
		c	18.318	15.693	38.261
ZN-29	Black shale	b	30.643	16.423	38.745
		c	33.571	16.578	39.145
ZN-30	Black shale	b	27.823	16.241	38.511
		c	29.114	16.311	38.497
ZN-32	Black shale	a	26.867	16.200	38.644
		b	25.880	16.121	38.504
		c	27.255	16.201	38.609
ZN-33	Black shale	a	21.515	15.876	38.202
		b	25.537	16.104	38.435
		c	29.644	16.350	39.244
ZN-34	Black shale	a	28.490	16.289	38.621
		b	30.986	16.412	38.628
		c	33.496	16.569	39.136
ZN-35	Black shale	a	25.459	16.097	38.531
		b	27.568	16.226	38.636
		c	30.528	16.405	39.030
ZN-35-1	Black shale	a	21.223	15.841	38.159
		b	24.693	16.045	38.410
		c	29.486	16.333	38.895
ZN-35-2	Black shale	a	20.540	15.804	38.080
		b	24.823	16.047	38.277
		c	28.883	16.303	38.554
HN-1	Ni–Mo sulfide ore	a	36.679	16.871	38.642
		b	35.206	16.761	38.615
		c	32.997	16.609	38.565
HN-2	Ni–Mo sulfide ore	a	38.276	16.936	38.598
		b	36.653	16.830	38.584
		c	33.270	16.616	38.548
GZ-1	Ni–Mo sulfide ore	a	94.156	20.195	38.880
		b	87.822	19.735	38.941
		c	44.977	17.238	38.492

respectively (Table 2). In contrast to the negative Eu and Ce anomaly of the black shales, some of the Ni–Mo–PGE–Au sulfide ores show positive Eu and Ce anomalies with Eu/Eu* up to 2.78 and Ce/Ce* up to 2.73 (Fig. 9, Table 2). All of the Ni–Mo sulfide samples display a positive Y anomaly, which is also in contrast to the variable Y anomaly in black shales (Fig. 9).

The positive Eu anomaly has been regarded as one of the characteristic features of modern and ancient massive

sulfide deposits of submarine hydrothermal exhalative origin (Graf 1977; Barrett et al. 1990; Peter and Goodfellow 1996; Jiang et al. 2000). Previous studies have shown that a positive Eu anomaly is not preserved in modern and ancient oxidized oceans because of the rapid oxidation of hydrothermal Eu²⁺ to Eu³⁺ in the water column, and any precipitates formed also strongly adsorb seawater REEs that lack a positive Eu anomaly (Peter and Goodfellow 1996). The negative Ce anomaly in the

Fig. 6 Concentrations of trace elements in black shales (**a**) and the Ni–Mo–PGE–Au sulfide ores (**b**). The values were normalized to average upper crust (AUC) (Rollinson 1993)



Niutitang black shales and the Ni–Mo–PGE–Au sulfide ores records a significant seawater component, similar to modern pelagic clays and modern deep-sea and metalliferous sediments (Piper and Graf 1974; Peter and Goodfellow 1996; Mills and Elderfield 1995; German

et al. 1999). Negative Ce anomalies appear to be common at modern submarine hydrothermal systems. The massive sulfide–sulfate samples from the Southern Explorer Ridge show relatively flat REE patterns with positive Eu and negative Ce anomalies (Barrett et al.

Fig. 7 Bivariate plots of trace elements: **a** Zr vs Hf, **b** Nb vs Ta, **c** Th vs Sc, **d** Ga vs Rb, **e** La vs Ce, **f** La vs Sm

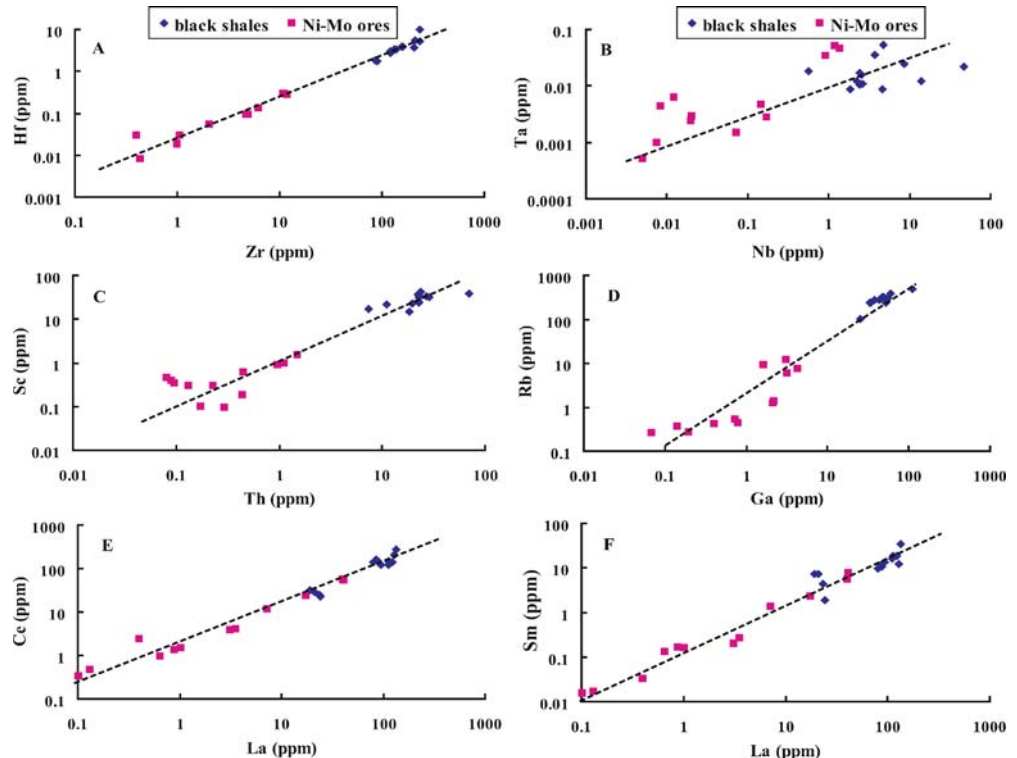


Fig. 8 Bivariate plots of trace elements: **a** Ba vs Sr, **b** Mn vs V, **c** Cu vs Zn, **d** U vs Mo, **e** V vs Mo, **f** Ni vs V

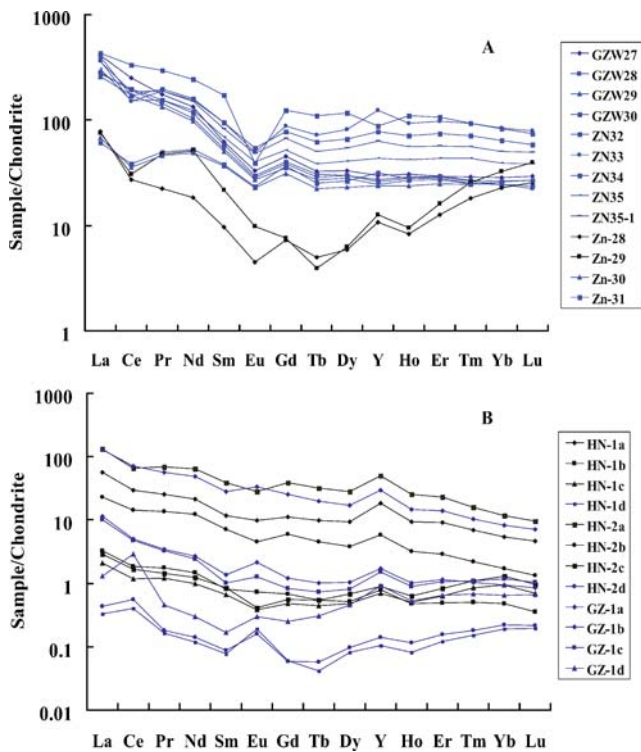
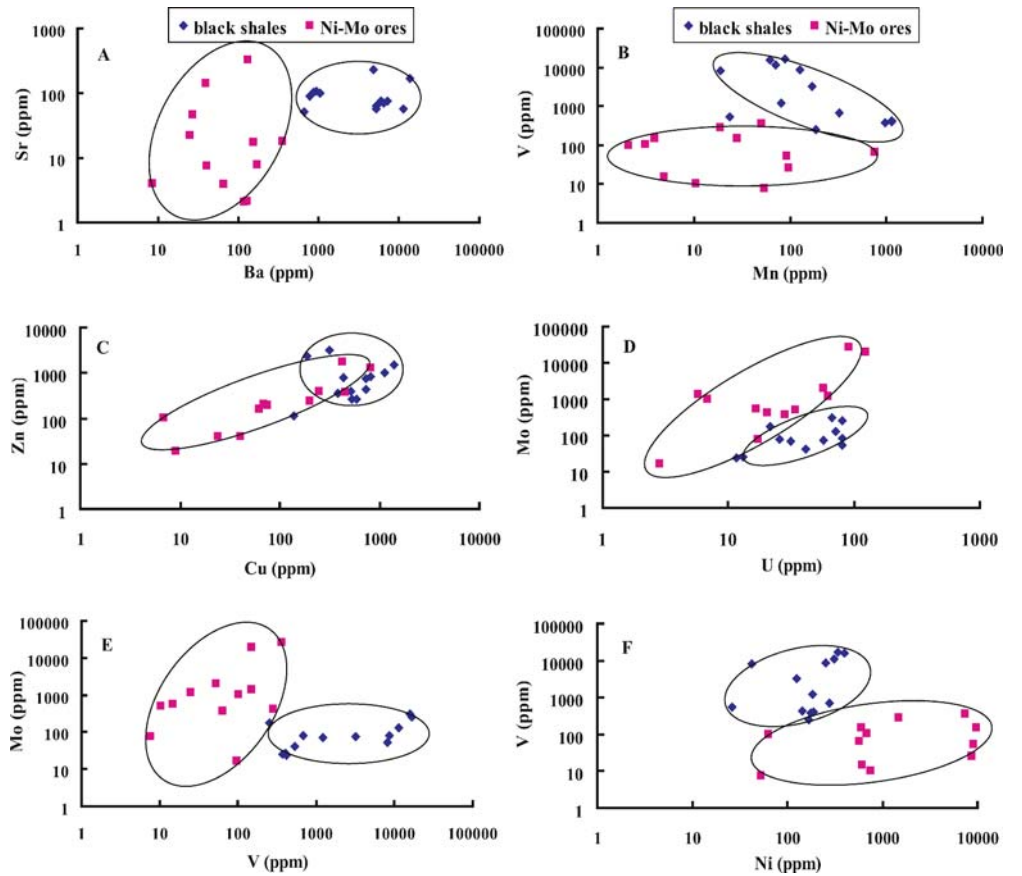


Fig. 9 Chondrite-normalized REE patterns of black shales (**a**) and Ni–Mo–PGE–Au sulfide ores (**b**) in the Lower Cambrian Niutitang Formation, South China

1990). Such REE patterns are also found in massive sulfides from Middle Valley on the Juan de Fuca Ridge (Krasnov et al. 1994) and oxides from the TAG mound (Mills and Elderfield 1995). The negative Ce anomalies in modern sulfide and oxide samples are best interpreted as resulting from variable mixing of hydrothermal fluid and seawater (Barrett et al. 1990; Mills and Elderfield 1995), based on the large negative Ce anomaly observed in seawater (Elderfield and Greaves 1982). Positive Ce anomalies have been reported for a few samples from anoxic waters of the Black Sea (Schijf et al. 1991). It has been suggested that the size of the Ce anomaly is mainly controlled by redox conditions and can be used as a tracer to distinguish between anoxic and oxic water bodies in the geological past (e.g., Elderfield and Greaves 1982; Shields and Stille 2001). Hence, the small positive Ce anomaly in several of our analyses may also reflect anoxic conditions.

Y and Ho are tightly coupled in many geochemical processes, leading to an invariable Y/Ho ratio of about 28 in common igneous rocks and clastic sediments (Bau 1996). However, modern seawater and submarine hydrothermal fluids are often characterized by non-chondritic Y/Ho ratios (Bau and Dulski 1999; Douville et al. 1999). In Fig. 10, most of the black shale samples show similar Y/Ho ratios, which are slightly higher than, but still close to those of igneous or clastic sedimentary rocks (~28); whereas, the Ni–Mo–PGE–Au sulfide ores display high Y/Ho ratios up to 60. The fractionation of Y and Ho is typical of aqueous

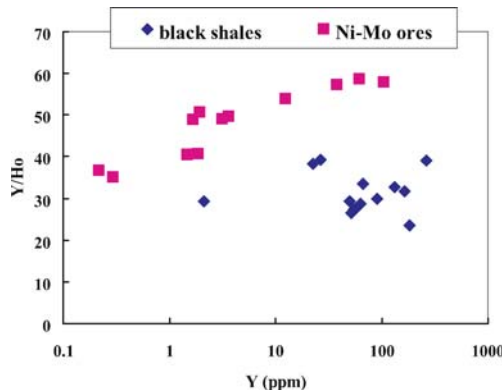


Fig. 10 Plot of Y vs Y/Ho ratios for black shales and Ni–Mo–PGE–Au sulfide ores in the Lower Cambrian Niutitang Formation, South China

environment; hence, the large Y/Ho ratios of the Ni–Mo–PGE–Au sulfide ores suggest that the REE source of the sulfide ores is dominated by aqueous REE complexes, rather than by terrigenous materials. In contrast, the REE in the black shales reflect mixing between terrigenous and aqueous sources, but the terrigenous source was dominant.

Discussion and conclusions

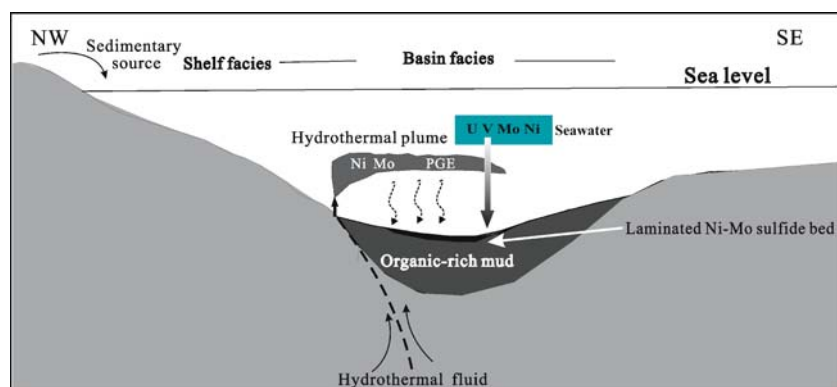
The ore genesis of the Ni–Mo–PGE–Au sulfide ores in the Lower Cambrian black shale sequence in the Yangtze Platform of south China has been long debated. It appears that two fluid phases may be responsible for the ore formation, i.e., seawater (Mao et al. 2002; Lehmann et al. 2003) and submarine hydrothermal fluids (Coveney et al. 1992; Lott et al. 1999; Steiner et al. 2001; Coveney 2003). Rare-earth elements, especially the Eu anomaly, have been used as a tracer to evaluate possible submarine hydrothermal inputs. Positive Eu anomalies are commonly found in ores and chemical precipitates associated with massive sulfide deposits. Previously, Steiner et al. (2001) have found positive Eu anomalies for the Ni–Mo–PGE–Au sulfide ores and their immediate footwall sulfidic shales of the Niutitang Formation, and suggested that this REE pattern recorded a mobilization of rare-earth elements by circulating hydrothermal fluids. It is believed that circulating hydrothermal fluids react with Eu-enriched feldspar-

bearing lithologies in the deep marine basin, which would mobilize Eu and, thus, cause a pronounced increase of Eu in the ore-forming solutions and their precipitates (e.g., Graf 1977). Positive Eu anomalies have also been found in the chert beds within the Lower Cambrian Niutitang black shale sequence, which is also an immediate host rock for the Ni–Mo–PGE–Au sulfide ores (Li and Gao 1996). Li and Gao (1996) suggested that these cherts were products of submarine hydrothermal exhalative origin.

In this study, we document positive Eu anomalies for some of the Ni–Mo–PGE–Au sulfide ores. In addition to the Eu anomaly, a comparison of the Ce and Y anomaly and Y/Ho ratios between the black shales and the Ni–Mo–PGE–Au sulfide ores is also in line with the submarine exhalative hydrothermal origin of the Ni–Mo–PGE–Au sulfide ores. Trace-element analysis of the black shales and the Ni–Mo–PGE–Au sulfide ores also indicates that hydrothermal inputs may contribute to the extreme enrichments of the redox-sensitive elements, base and precious metals, and many other metals, such as Sr and Ba, whereas immobile elements, such as high-field-strength elements, redox-insensitive rare-earth elements, and Rb and Ga, are not derived from hydrothermal sources; rather, they may come from terrigenous sources.

There are many other lines of geological and geochemical evidence that support the interpretation in favor of a hydrothermal origin for the Ni–Mo–PGE–Au sulfide ores in the Lower Cambrian black shale sequence in South China. For example, Murowchick et al. (1994) revealed a wide $\delta^{34}\text{S}$ range from +22 to –26‰ for the sulfide nodules, suggestive of bacterial reduction of seawater sulfate in an anoxic, phosphogenic, and metallogenic basin. These authors suggested that intermittent venting of metal-laden hydrothermal fluids into such a bacteriogenic sulfide-rich environment resulted in precipitation of metal sulfides as pseudomorphous replacements of organic debris and as sulfide sediments that recorded cyclic, large sulfur isotope variations (Murowchick et al. 1994). Lott et al. (1999) identified footwall quartz-sulfide stock works about 10 m below the Ni–Mo sulfide ore bed and measured fluid inclusion homogenization temperatures up to 290°C for these veins. These crosscutting vein relations are consistent with a hydrothermal model with fluids leaking through stock work veins that supplied ore constituents to the

Fig. 11 A genetic model for the formation of the Ni–Mo–PGE–Au sulfide ores in the Lower Cambrian black shale sequence in South China



seafloor, leading to ore precipitation and preservation within isolated basins on the seafloor (Coveney 2003).

Besides the polymetallic Ni–Mo–PGE–Au sulfide ores hosted in the Lower Cambrian strata, other mineralizations also occur within the same strata in South China, such as stratiform barite, massive phosphorite and manganese carbonates (Wang and Li 1991; Coveney et al. 1994; Hein et al. 1999; Clark et al. 2004). In particular, the barite mineralization has been proposed as of typical submarine hydrothermal origin by many researchers, because the deposits display all the geologic characteristics and radiogenic/stable isotopic compositions of other Palaeozoic barite deposits that are of hydrothermal origin (Peng et al. 1999; Wu et al. 1999; Fang et al. 2002; Clark et al. 2004). The occurrence of submarine hydrothermal barite deposits establishes that the Early Cambrian was a period of intense hydrothermal venting along the entire margin of the Yangtze Platform (Clark et al. 2004; Emsbo et al. 2005).

In conclusion, we suggest that the Ni–Mo–PGE–Au sulfide ores in the Lower Cambrian Niutitang black shale sequence may have formed via submarine hydrothermal exhalation. Figure 11 represents a summary and a general genetic model proposed for these black-shale-hosted Ni–Mo–PGE–Au sulfide ore deposits in south China. The establishment of submarine hydrothermal activity in the Early Cambrian ocean is of importance not only from an economic geology point of view with identification of a new type of ore deposit, but also it may have profound implications for the metazoan diversification in the Early Cambrian sea on the Yangtze Platform.

Acknowledgements This research was supported by China National Science Foundation grants (40221301, 40372059, 40232020). Profs. Zhu Maoyan, Zhang Junming, and Wu Xianhe are thanked for their very helpful assistance in field work and for critical discussions. We thank Dr. R. M. Coveney Jr., J. B. Murowchick J.B., and an anonymous reviewer for their constructive comments that helped us to better clarify our view and improve the paper significantly.

References

- Anderson RF, Fleisher MQ, LeHuray AP (1989) Concentration, oxidation state, and particulate flux of uranium in the Black Sea. *Geochim Cosmochim Acta* 53:2215–2224
- Barfod GH, Albarède F, Knoll AH, Xiao S, Telouk P, Frei R, Baker J (2002) New Lu–Hf and Pb–Pb age constraints on the earliest animal fossils. *Earth Planet Sci Lett* 201:203–212
- Barrett TJ, Jarvis I, Jarvis KE (1990) Rare earth element geochemistry of massive sulfides–sulfates and gossans on the Southern Explorer Ridge. *Geology* 18:583–586
- Bau M (1996) Controls on the fractionation of isovalent trace elements in magmatic and aqueous systems: evidence from Y/Ho, Zr/Hf, and lanthanide tetrad effect. *Contrib Mineral Petrol* 123:323–333
- Bau M, Dulski P (1999) Comparing yttrium and rare earths in hydrothermal fluids from the Mid-Atlantic Ridge: implications for Y and REE behavior during near-vent mixing and for the Y/Ho ratio of Proterozoic seawater. *Chem Geol* 155:77–90
- Bros R, Stille P, Gauthier-Lafaye F, Weber F, Clauer N (1992) Sm–Nd isotopic dating of Proterozoic clay materials: an example from the Francevillian sedimentary series, Gabon. *Earth Planet Sci Lett* 113:207–218
- Canet C, Alfonso P, Melgarejo JC, Belyatsky BV (2004) Geochemical evidences of sedimentary-exhalative origin of the shale-hosted PGE–Ag–Au–Zn–Cu occurrences of the Prades Mountains (Catalonia, Spain): trace-element abundances and Sm–Nd isotopes. *J Geochem Explor* 82:17–33
- Chen YQ, Jiang SY, Ling HF, Feng HZ, Yang JH, Chen JH (2003) Pb–Pb isotope dating of black shales from the Lower Cambrian Niutitang Formation, Guizhou Province, South China. *Prog Nat Sci* 13:771–776
- Chen DF, Dong WQ, Zhu BQ, Chen XP (2004) Pb–Pb ages of Neoproterozoic Doushantuo phosphorites in South China: constraints on early metazoan evolution and glaciation events. *Precambrian Res* 132:123–132
- Clark SB, Poole FG, Wang Z (2004) Comparison of some sediment-hosted, stratiform barite deposits in China, the United States, and India. *Ore Geol Rev* 24:85–101
- Clauer N (1981) Rb–Sr and K–Ar dating of Precambrian clays and glauconites. *Precambrian Res* 15:331–352
- Cooper JR, Daasch EJ, Kaye M (1974) Isotope and elemental geochemistry of Black Sea sediments. In: Degens ET, Ross DA (eds.) *The Black Sea*. Am Assoc Pet Geol Mem 20:554–565
- Coveney RM Jr (2003) Re–Os dating of polymetallic Ni–Mo–PGE–Au mineralization in Lower Cambrian black shales of South China and its geological significance—a discussion. *Econ Geol* 98:661–662
- Coveney RM Jr, Murowchick JB, Grauch RI, Michael D, Glascock D, Denison JD (1992) Gold and platinum in shales with evidence against extraterrestrial sources of metals. *Chem Geol* 99:101–114
- Coveney RM Jr, Grauch RI, Murowchick JB (1994) Metals, phosphate and stone coal in the Proterozoic and Cambrian of China: the geologic setting of precious metal-bearing Ni–Mo ore beds. *Society of Economic Geologists Newsletter* 18:1–11
- Douville E, Bienvenu P, Charlou JI, Donval JP, Fouquet Y, Appriou P, Gamo T (1999) Yttrium and rare earth elements in fluids from various deep-sea hydrothermal systems. *Geochim Cosmochim Acta* 63:627–643
- Elderfield H, Greaves MJ (1982) The rare earth elements in seawater. *Nature* 296:214–219
- Emsbo P, Hofstra AH, Johnson CA, Koenig A, Grauch R (2005) Lower Cambrian metallogenesis of South China: interplay between diverse basinal hydrothermal fluids and marine chemistry. In: Mao J and Bierlein FP (eds.) *Mineral deposit research: meeting the global challenge*, Proceedings of the 8th Biennial SGA meeting, Beijing, China. Springer, Berlin Heidelberg New York, pp 115–118
- Fan D (1983) Polyelements in the Lower Cambrian black shale series in southern China. In: Augustithis SS (ed) *The significance of trace elements in solving petrogenetic problems and controversies*. Theophrastus, Athens, pp 447–474
- Fan D, Yang X, Wang Y, Chen N (1973) Petrological and geochemical characteristics of a nickel–molybdenum–multi-element-bearing Lower Cambrian black shale from a certain district in south China. *Geochimica* 3: 143–163 (in Chinese)
- Fan D, Yang R, Huang Z (1984) The Lower Cambrian black shales series and the iridium anomaly in south China. In: *Development in Geoscience*, 27th International Geology Congress, Moscow 1984. Beijing Science, pp 215–224
- Fang WX, Hu RZ, Su WC (2002) Geochemical characteristics of Dahebiang-Gongxi superlarge barite deposits and its background of tectonic geology, China. *Acta Petrolei Sinica* 18 (2):247–256
- Galer SJG, O’Nions RK (1989) Chemical and isotopic studies of ultramafic inclusions from the San Carlos volcanic field, Arizona: a bearing on their petrogenesis. *J Petrol* 30:1033–1064

- Gauthier-Lafaye F, Bros R, Stille P (1996) Pb-Pb isotope systematics on diagenetic clays: an example from Proterozoic black shales of the Franceville basin (Gabon). *Chem Geol* 133:243–250
- German CR, Hergt J, Palmer MR, Edmond JM (1999) Geochemistry of a hydrothermal sediment core from the OBS vent-field, 21° N East Pacific Rise. *Chem Geol* 155:65–75
- Goodfellow WD, Jonasson IR (1986) Environment of formation of the Howards Pass (XY) Zn-Pb deposit, Selwyn Basin, Yukon. In: Morin JA (ed) *Mineral deposits of the Northern Cordillera. CIM Spec Vol* 37:19–50
- Gradstein FM, Ogg JG, Smith AG, Bleeker W, Lourens LJ (2004) A new geologic time scale with special reference to Precambrian and Neogene. *Episodes* 27(2):83–100
- Graf JL Jr (1977) Rare earth elements as hydrothermal tracers during the formation of massive sulfide deposits in volcanic rocks. *Econ Geol* 72:527–548
- Hein JR, Fan D, Ye J, Liu T, Yeh H-W (1999) Composition and origin of Early Cambrian Tiantaishan phosphorite-Mn carbonate ores, Shaanxi Province, China. *Ore Geol Rev* 15:95–134
- Hirst DM (1974) Geochemistry of sediments from eleven Black Sea cores. In: Degens ET, Ross DA (eds) *The Black Sea: geology, chemistry, and biology*. American Association of Petroleum Geologists Memoir, Tulsa, Oklahoma, pp 430–455
- Holland HD (1979) Metals in black shales—a reassessment. *Econ Geol* 74:295–314
- Horan MF, Morgan JW, Grauch RI, Coveney RM Jr, Murowchick JB, Hulbert LJ (1994) Rhenium and osmium isotopes in black shales and Ni-Mo-PGE-rich sulfide layers, Yukon Territory, Canada, and Hunan and Guizhou Provinces, China. *Geochim Cosmochim Acta* 58:257–265
- Jenkins RJF, Cooper JA, Compston W (2002) Age and biostratigraphy of Early Cambrian tuffs from SE Australia and southern China. *J Geol Soc (Lond)* 159:645–658
- Jiang S-Y, Han F, Shen J-Z, Palmer MR (1999) Chemical and Sr-Nd isotopic systematics of tourmaline from the Dachang Sn-polymetallic ore deposit, Guangxi Province, China. *Chem Geol* 157:49–67
- Jiang S-Y, Palmer MR, Slack JF, Yang J-H, Shaw D R (2000) Trace element and rare earth element geochemistry of tourmaline from the Sullivan Pb-Zn-Ag deposit and regional tourmalinites. In: Lydon JW, Hoy T, Slack JF, Knapp ME (eds) *The geological environment of the Sullivan deposit, British Columbia*. Geol Assoc Can 1:482–495 (Spec publication)
- Jiang S-Y, Yang J-H, Ling H-F, Feng H-Z, Chen Y-Q, Chen J-H (2003) Re-Os isotopes and PGE geochemistry of black shales and intercalated Ni-Mo polymetallic sulfide bed from the Lower Cambrian Niutitang Formation, South China. *Prog Nat Sci* 13:788–794
- Jiang S-Y, Wang R-C, Xu X-S, Zhao K-D (2005) Mobility of high field strength elements (HFSE) in magmatic-, metamorphic-, and submarine-hydrothermal systems. *Phys Chem Earth Parts A/B/C* 30(17–18):1020–1029
- Kao LS, Peacor DR, Coveney RM Jr, Zhao G, Dungey KE, Curtis MD, Penner-Hahn JE (2001) A C/MoS₂ mixed-layer phase (MoSC) occurring in metalliferous black shales from southern China, and new data on jordisite. *Am Mineral* 86:852–861
- Krasnov S, Stepanova T, Stepanov M (1994) Chemical composition and formation of a massive sulfide deposit, Middle Valley, northern Juan de Fuca Ridge (Site 856). In: Mottl MJ, Davis EE, Fisher AT, Slack JF (eds) *Proceedings of the ocean drilling program, scientific results, Middle Valley area, northeast Pacific Ocean: College Station, Texas, Ocean Drilling Program*, 139:353–372
- Li S, Gao Z (1996) Siliceous rocks of hydrothermal origin in the Lower Cambrian black rock series of South China. *Acta Mineral Sinica* 16:416–422 (in Chinese)
- Li S, Gao Z (1999) Study of noble metal enrichment in Lower Cambrian black rock series of Guizhou-Hunan Provinces, China. *J China Univ Geosci* 10:89–92
- Li S-R, Xiao Q-Y, Shen J-F, Sun L, Liu B, Yan B-K (2002) Source of Lower Cambrian platinum group elements in black shales in Hunan and Guizhou provinces, China and the Re-Os isotope dating. *Sci China (Ser D)* 32:568–575
- Lehmann B, Mao J, Li S, Zhang G, Zeng M (2003) Re-Os dating of polymetallic Ni-Mo-PGE-Au mineralization in Lower Cambrian black shales of South China and its geological significance—a reply. *Econ Geol* 98:663–665
- Lott DA, Coveney RM Jr, Murowchick JB (1999) Sedimentary exhalative nickel-molybdenum ores in South China. *Econ Geol* 94:1051–1066
- Lottermoser BG (1989) Rare earth element study of exhalites within the Willyama Supergroup, Broken Hill Block, Australia. *Miner Depos* 24:92–99
- Mao J, Lehmann B, Du A, Zhang G, Ma D, Wang Y, Zeng M, Kerrich R (2002) Re-Os dating of polymetallic Ni-Mo-PGE-Au mineralization in Lower Cambrian black shales of South China and its geologic significance. *Econ Geol* 97:1051–1061
- McLennan SM (1989) Rare earth elements in sedimentary rocks: influence of provenance and sedimentary processes. *Rev Mineral Geochem* 21:169–200
- Mills RA, Elderfield H (1995) Rare earth element geochemistry of hydrothermal deposits from the active TAG mound, 26 °N Mid-Atlantic Ridge. *Geochim Cosmochim Acta* 59:3511–3524
- Murowchick JB, Coveney RM Jr, Grauch RI, Chen Nancheng (1992) Ni-Mo ores of southern China: biologic, tectonic and sedimentary controls on their origin. In: 29th International Geology Congress, Abstr 3:2997
- Murowchick JB, Coveney RM Jr, Grauch RI, Eldridge CS, Shelton KL (1994) Cyclic variations of sulfur isotopes in Cambrian stratobound Ni-Mo-(PGE-Au) ores of southern China. *Geochim Cosmochim Acta* 58:1813–1823
- Pasava J (1993) Anoxic sediments - an important environment for PGE: an overview. *Ore Geol Rev* 8:425–445
- Peng J, Xia WJ, Yi HS (1999) Geological and geochemical characteristics and genesis of the Gongxi barite deposit, Xinhuan county, Hunan province. *J Chengdu Univ Tech* 26 (1):92–96 (in Chinese)
- Peter JM, Goodfellow WD (1996) Mineralogy, bulk and rare earth element geochemistry of massive sulphide-associated hydrothermal sediments of the Brunswick horizon, Bathurst mining camp, New Brunswick. *Can J Earth Sci* 33:252–283
- Piper DZ, Graf PA (1974) Gold and rare earth elements in sediments from the East Pacific Rise. *Mar Geol* 17:287–297
- Quip Y, Gao S, McNaughton NJ, Groves DI, Ling W (2000) First evidence of >3.2 Ga continental crust in the Yangtze craton of south China and its implications for Archean crustal evolution and Phanerozoic tectonics. *Geology* 28:11–14
- Quinby-Hunt MS, Wilde P (1994) Thermodynamic zonation in the black shale facies based on iron-manganese-vanadium content. *Chem Geol* 113:297–317
- Rollinson HR (1993) *Using geochemical data: evaluation, presentation, interpretation*. Longman Scientific Technical, Harlow, United Kingdom, pp 343
- Schijf J, de Baar HJW, Wijbrans JR, Landing WM (1991) Dissolved rare earth elements in the Black Sea. *Deep-Sea Res* 38 (Suppl 2):S805–S823
- Shields G, Stille P (2001) Diagenetic constraints on the use of cerium anomalies as paleoseawater redox proxies: an isotope and REE study of Cambrian phosphorites. *Chem Geol* 175:29–48
- Slack JF, Hoy T (2000) Geochemistry and provenance of clastic metasedimentary rocks of the Aldridge and Fort Steele Formations, Purcell Supergroup, southeastern British Columbia. In: Lydon JW, Hoy T, Slack JF, Knapp ME (eds) *The geological environment of the Sullivan Deposit, British Columbia*, Geol Assoc Can 1:180–201(Special publication)
- Stille P, Clauer N (1986) Sm-Nd isochron age and provenance of the argillites of the Gunflint Iron Formation in Ontario, Canada. *Geochim Cosmochim Acta* 50:1141–1146

- Steiner M, Willis E, Erdtmann BD, Zhao YL, Yang RD (2001) Submarine-hydrothermal exhalative ore layers in black shales from South China and associated fossils- insights into a Lower Cambrian facies and bio-evolution. *Palaeogeogr Palaeoclimatol Palaeoecol* 169:165–191
- Taylor SR, McLennan SM (1985) The continental crust: its composition and evolution. Blackwell, Oxford
- Todt W, Cliff RA, Hanser A, Hofmann AW (1996) Re-calibration of NBS lead standards using a ^{202}Pb + ^{205}Pb double spike. In: Basu A, Hart S (eds.) Earth processes: reading the isotopic cod. *Geophys Monogr* 95:429–437
- Toyoda K, Masuda A (1991) Chemical leaching of pelagic sediments: identification of the carrier of Ce anomaly. *Geochem J* 25:95–119
- Wang Z, Li G (1991) Baryte and witherite deposits in Lower Cambrian shales of South China: stratigraphic distribution and geochemical characterization. *Econ Geol* 86:354–363
- Whitehead RES, Davies JF, Goodfellow WD (1992) Lithogeochemical patterns related to sedex mineralization, Sudbury Basin, Canada. *Chem Geol* 98:87–101
- Wignall PB (1994) Black shales. Clarendon, Oxford, pp 127
- Wu C-D, Yang C-Y, Chen Q-Y (1999) The hydrothermal sedimentary genesis of barite deposits in west Hunan and east Guizhou. *Peking Univ (Acta Sci Natur)* 36(6):774–785 (in Chinese)
- Yarincik KM, Murray RW, Lyons TW, Peterson LC, Haug GH (2000) Oxygenation history of bottom waters in the Cariaco Basin, Venezuela, over the past 578,000 years: results from redox-sensitive metals (Mo, V, Mn, and Fe). *Paleoceanography* 15:593–604
- Yin CY, Tang F, Liu YQ, Gao LZ, Liu PJ, Xing YS, Yang ZQ, Wan YS, Wang ZQ (2005) U-Pb zircon age from the base of the Ediacaran Doushantuo Formation in the Yangtze Gorges, South China: constraint on the age of Marinoan glaciation. *Episodes* 28:48–49
- Zhang S, Jiang G, Zhang J, Song B, Kennedy MJ, Christie-Blick N (2005) U-Pb sensitive high-resolution ion microprobe ages from the Doushantuo Formation in south China: constraints on late Neoproterozoic glaciations. *Geology* 33:473–476
- Zeng MA (1998) Geological features of the Huangjiawan Ni-Mo deposit in Zunyi of Guizhou and its prospect for development. *Guizhou Geol* 16:305–310 (in Chinese)
- Zhu M (2004) Introduction to biological and geological processes of the Cambrian explosion: evidence from the Yangtze Platform of South China. In: Zhu M and Steiner M (eds) Biological and geological processes of the Cambrian explosion. *Progr Nat Sci*, pp V–X (Special issue)